

Storage Ring Measurement of Electric Dipole Moments of Protons and Other Baryons

April 23, 2012

Richard Talman
Laboratory of Elementary-Particle Physics
Cornell University

Abstract

Electric dipole moment (EDM) measurements may help to answer the question “**Why is there more matter than antimatter in the present universe?**”. For a charged baryon like the proton such a measurement is thinkable only in a ring in which a bunch of protons is stored for more than a few minutes, with **polarization “frozen”** (relative to the beam velocity) and with the **polarization not attenuated by decoherence**. Lattices with these capabilities are described, including one, as an all-electric example, situated in the Tevatron accumulator tunnel. Rings for later measurements of other charged baryons, such as the deuteron or helium-3 nuclei, are more complicated. ”Precursor” experiments are also described in which an electrostatic separator borrowed from the Tevatron is used as a prototype bending element in the COSY ring in Juelich Germany.

Contents

1	Theoretical Motivation	3
2	Symmetry Violations for a Particle with both MDM and EDM	4
3	EDM-Induced Spin Precession Estimate	5
4	Spin Precession Due to MDM and EDM in All-Electric Ring	6
4.1	MDM-Induced Precession	6
4.2	EDM-Induced Precession	6
5	Frozen Spin Requirements	7
6	Some Possible Ring Lattice Designs	10
6.1	All-electric Proton Ring	10
6.2	“All-In-One” Lattice for Measuring p, d, and ^3He	14
6.3	All-electric Ring In Tevatron Accumulator Tunnel	17
7	COSY Storage Ring Test Using Tevatron Electrostatic Separator	21
8	Essentials for any Hadron EDM Measurement	23
9	Orbits in Electric Fields	27
9.1	Synchro-Betatron Coupling	27
9.2	“Exact” Tracking with UAL/ETEAPOT Code	29
10	Estimation of Spin Coherence Time (SCT)	32

1 Theoretical Motivation

- J. R. Ellis, M. K. Gaillard, D. V. Nanopoulos, and S. Rudaz, *A Cosmological Lower Bound on the Neutron Electric Dipole Moment*, Phys.Lett. B99 (1981) 101. “We argue that in a wide class of grand unified theories diagrams similar to those generating baryon number in the early universe also contribute to renormalization of the CP-violating θ parameter of QCD and hence to the neutron electric dipole moment d_n . We then deduce an order-of-magnitude **lower bound on the neutron electric dipole moment: $d_n \approx 3 \times 10^{-28}$ e cm.**”
- S. Weinberg, Conference summary (HEP Dallas conference 1992), AIP Conf. “Also endemic in supersymmetry theories are CP violations that go beyond the CKM matrix, and for this reason it may be that the next exciting thing to come along will be the discovery of a neutron or atomic or electron electric dipole moment. These **electric dipole measurements seem to me to offer one of the most exciting possibilities for progress in particle physics.**”
- The 2007 NSAC Long Range Plan emphasized the **importance of electric dipole moment (EDM) measurements** for answering the question “**Why is there more matter than antimatter in the present universe?**”. At that time it was the neutron that seemed to be the most promising candidate for this measurement. Subsequent studies have suggested that proton, deuteron, and helium-3 EDM’s can be measured, using storage rings, to greater precision than neutrons.
- In his introductory talk, *Pushing Beyond the LHC*, at the 2011 Fundamental Physics at the Intensity Frontier Conference, in Rockville MD, Arkani-Hamed identified **EDM’s (along with quark and lepton flavor physics) as the areas of greatest promise.**

2 Symmetry Violations for a Particle with both MDM and EDM

- Visualize a magnetic dipole as a loop of current lying in a plane; it is a (pseudo-)vector normal to the plane.
- Visualize an electric dipole as a vector pointing from positive to negative charge.
- With their axes aligned, both define the same plane. But they are not geometrically equivalent. The electric vector differentiates between the two sides of the plane but does not determine an in-plane rotational sense. The magnetic pseudo-vector determines an in-plane rotational sense, but does not distinguish between the two sides of the plane.
- **ED and MD cannot be said to be “parallel” without violating parity P.** Viewed in a mirror ED and MD would be anti-parallel.
- **For ED and MD to be said to be “parallel” also violates time reversal T.** Run backwards MD would reverse, ED would not.

3 EDM-Induced Spin Precession Estimate

- With polarization “frozen” parallel to particle momentum, any radial electric field acting on the EDM causes the polarization to precess up or down.
- Numerically, in SI units, we can define a “nominal” electric dipole moment $\tilde{d}_{\text{nom}} = 10^{-29} \cdot (1.602 \times 10^{-19}) \cdot (0.01) = (1.602 \times 10^{-50})$ [SI]. **At our most optimistic, an EDM of 10^{-29} can be persuasively distinguished from zero in one year of running.**
- The EDM/MDM ratio $\tilde{d}_{\text{nom}}/\mu_B = (1.602 \times 10^{-50})/(5.05 \times 10^{-27}) = 3.127 \times 10^{-24}$, with both numerator and denominator in SI units. This ratio is not dimensionless and cannot therefore be used to estimate the relative strength of electric and magnetic precession. The missing factor is E/B . For our configurations, in SI units, this ratio is typically $10^7/0.1 \approx 10^8$. After multiplying by this factor, the **relative-effectiveness ratio** *is* dimensionless and has a numerical value of about $\mathbf{3} \times \mathbf{10}^{-16}$. This is the factor by which the EDM-induced precession is smaller than the MDM-induced precession.
- Fortunately the magnetic precession is quite large, of order 2π per turn which, at one microsecond per turn, is almost 10^7 radians/s. We therefore have to plan to measure a “nominal” EDM-induced precession of order 10^{-9} r/s. After 10^5 s this would be 0.1 mr.

4 Spin Precession Due to MDM and EDM in All-Electric Ring

The rest frame electric and magnetic field vectors \mathbf{E}' and \mathbf{B}' are given in terms of lab frame vectors by

$$\mathbf{E}' = \gamma(\mathbf{E} + \boldsymbol{\beta} \times c\mathbf{B}) = -\gamma(E + \beta cB) \hat{\mathbf{x}} \quad (1)$$

$$\mathbf{B}' = \gamma(\mathbf{B} - \boldsymbol{\beta} \times \mathbf{E}/c) = \gamma(B + \beta E/c) \hat{\mathbf{y}}. \quad (2)$$

The simplifications have resulted from the laboratory magnetic field \mathbf{B} having only a (vertical) y -component, and $\boldsymbol{\beta}$ and \mathbf{E} having only horizontal components. As a result, in the rest frame, the electric field is horizontal and the magnetic field is vertical.

4.1 MDM-Induced Precession

A particle at rest, with angular momentum \mathbf{s}' and magnetic dipole moment $g\mu_B\mathbf{s}'$, in magnetic field \mathbf{B}' , is subject to torque $g\mu_B\mathbf{s}' \times \mathbf{B}'$;

$$\frac{d\mathbf{s}'}{dt'} = -g\mu_B\mathbf{B}' \times \mathbf{s}' = -g\mu_B\gamma(\beta E/c) \hat{\mathbf{y}} \times \mathbf{s}'. \quad (3)$$

With \mathbf{s}' horizontal, **the precession is horizontal.**

4.2 EDM-Induced Precession

The precession occurring in an all-electric ring satisfies

$$\left. \frac{d\mathbf{s}'}{dt'} \right|_{\text{EDM,E}} = \tilde{d} E \gamma \hat{\mathbf{x}} \times \mathbf{s}'. \quad (4)$$

With \mathbf{s}' horizontal, **the precession is vertical.** This is the precession that has to be measured to obtain EDM \tilde{d} .

5 Frozen Spin Requirements

The proton, deuteron, and helium MDM anomalies are:

$$\begin{aligned} G_p &= 1.7928473565 \\ G_d &= -0.14298727202 \\ G_{3\text{He}} &= -4.1839627399 \end{aligned} \quad (5)$$

With θ being angular position in ring and α the polarization angle, the **spin tunes** of all-magnetic and all-electric lattices are given by

$$Q_M \equiv \left. \frac{d\alpha}{d\theta} \right|_M = \gamma G, \quad Q_E \equiv \left. \frac{d\alpha}{d\theta} \right|_E = G\beta^2\gamma - \frac{1}{\gamma}. \quad (6)$$

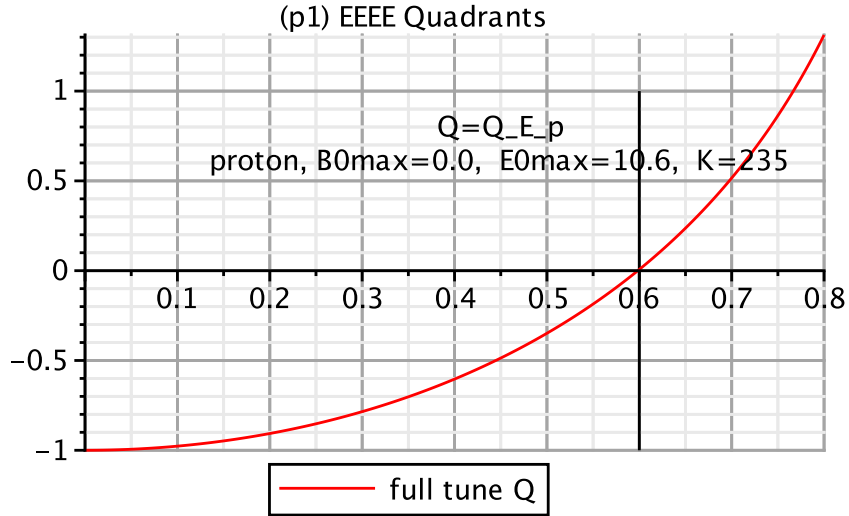


Figure 1: β -dependence of (magnetic) spin tune Q_M for protons in all-electric lattice. The spin is “**globally frozen**” for $\beta=0.6$.

$$Q_M = \gamma G, \quad Q_E = G\beta^2\gamma - \frac{1}{\gamma}. \quad (7)$$

$$G_d = -0.14298727202 \quad (8)$$

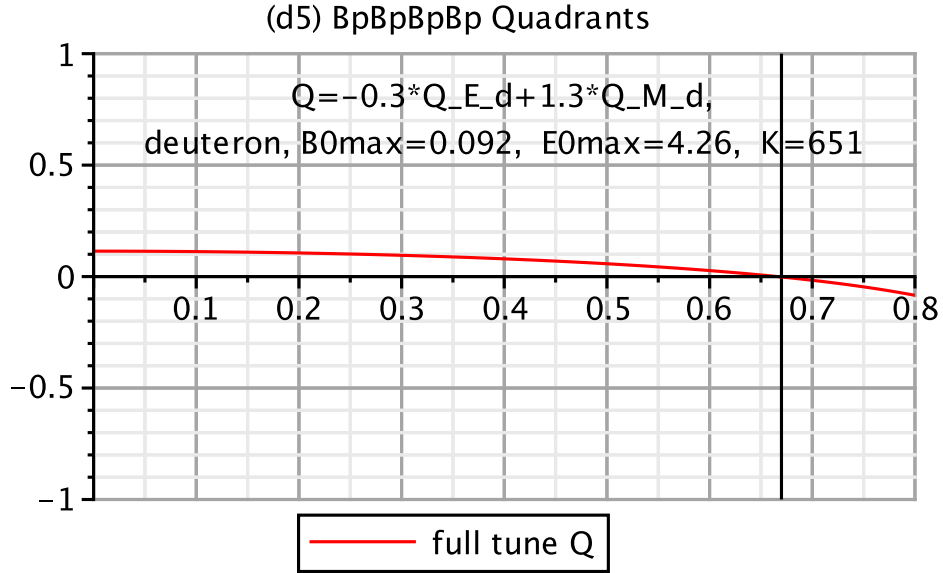


Figure 2: β -dependence of (magnetic) spin tune Q_M for deuterons in an electric/magnetic superimposed lattice. The spin is “**globally frozen**” for $\beta=0.67$.

$$G_p = 1.7928473565 \quad (9)$$

$$Q_M = \gamma G, \quad (10)$$

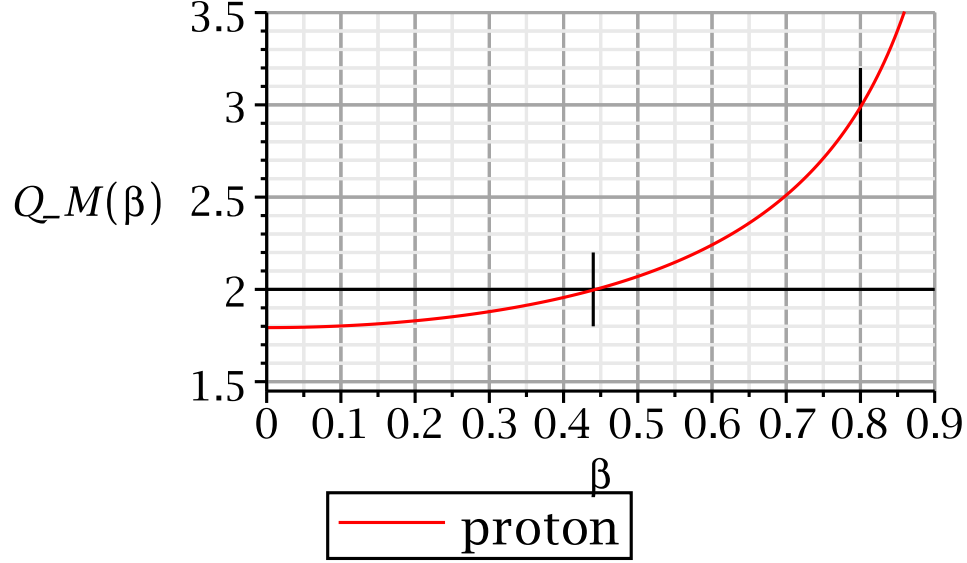


Figure 3: β -dependence of (magnetic) spin tune Q_M for protons. The spin is “**locally frozen**” (spin tune is non-zero integer) for $\beta=0.44$, kinetic energy $K=0.1066$ GeV; and for $\beta=0.80$, $K=0.6255$ GeV. This configuration is achievable at the existing COSY ring. 10^{-27} e-cm EDM measurement accuracy might be possible.

6 Some Possible Ring Lattice Designs

6.1 All-electric Proton Ring

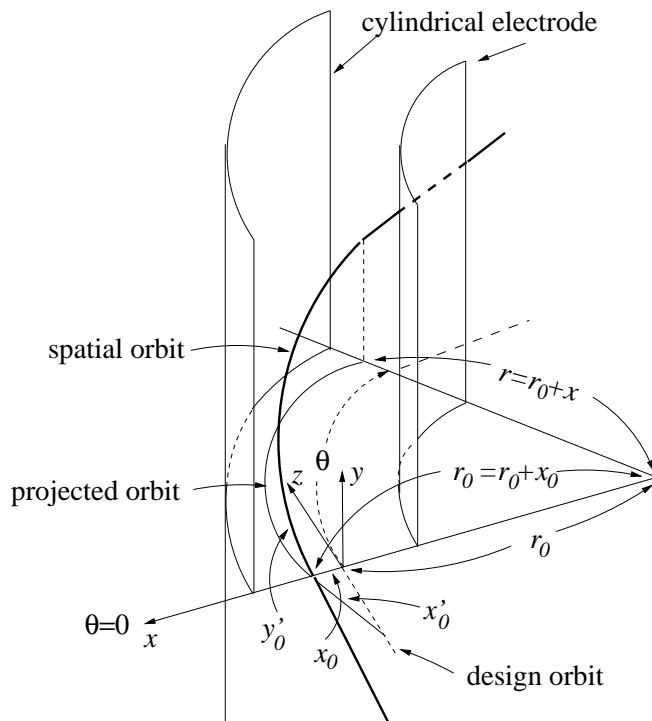


Figure 4: The bold curve shows a proton orbit passing through a curved-planar cylindrical electrostatic bending element. The electrode spacing is g and the design orbit is centered between the electrodes.

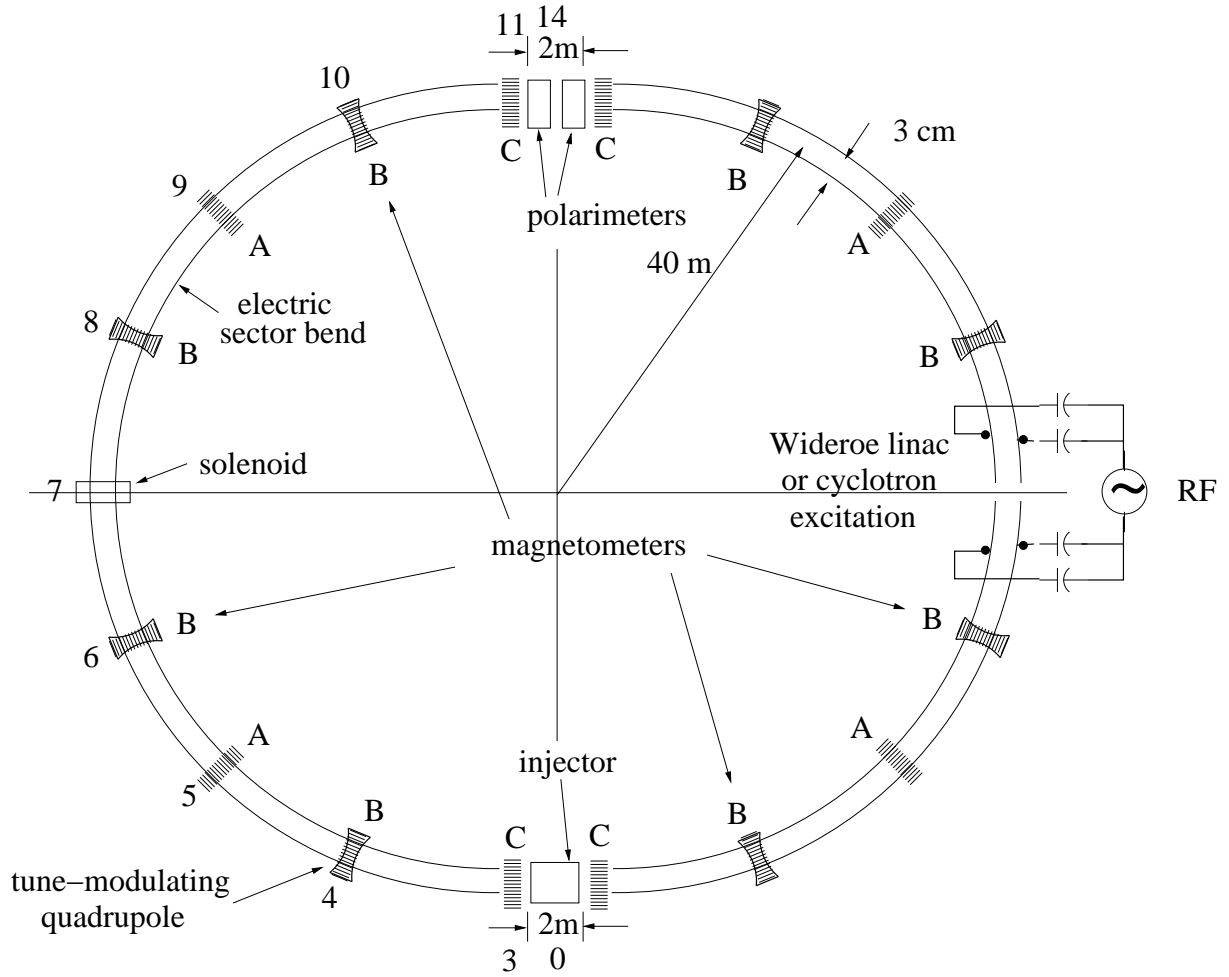


Figure 5: A very weak focusing all-electric lattice for measuring the electric dipole moment of the proton. Electric quadrupoles at the B locations tune the vertical tune to, for example, $Q_{y,0} = 0.2$, and wobble Q_y from that value for synchronous detection of the vertical beam positions at A and C locations.

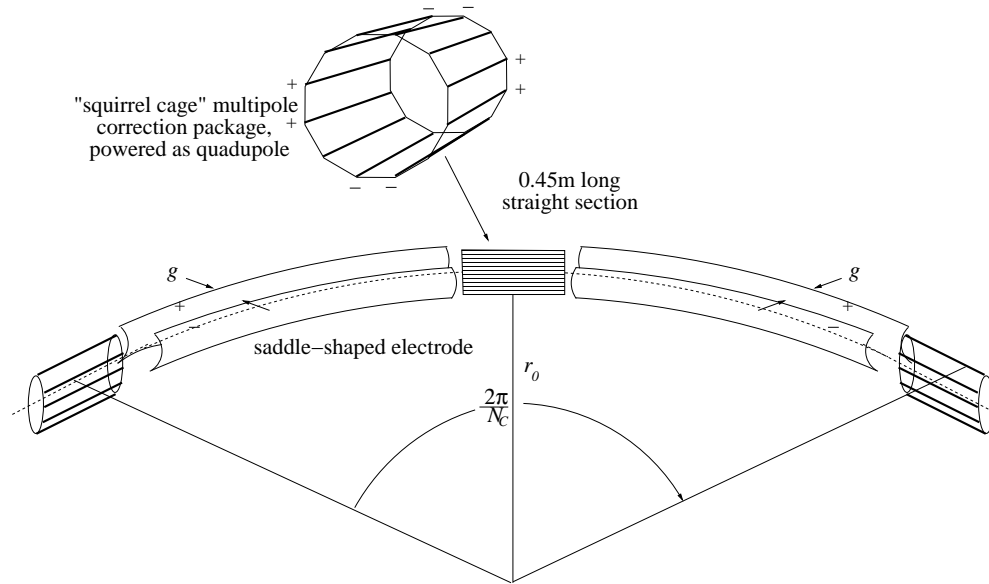


Figure 6: Sketch of one cell of baseline all-electric proton EDM lattice.

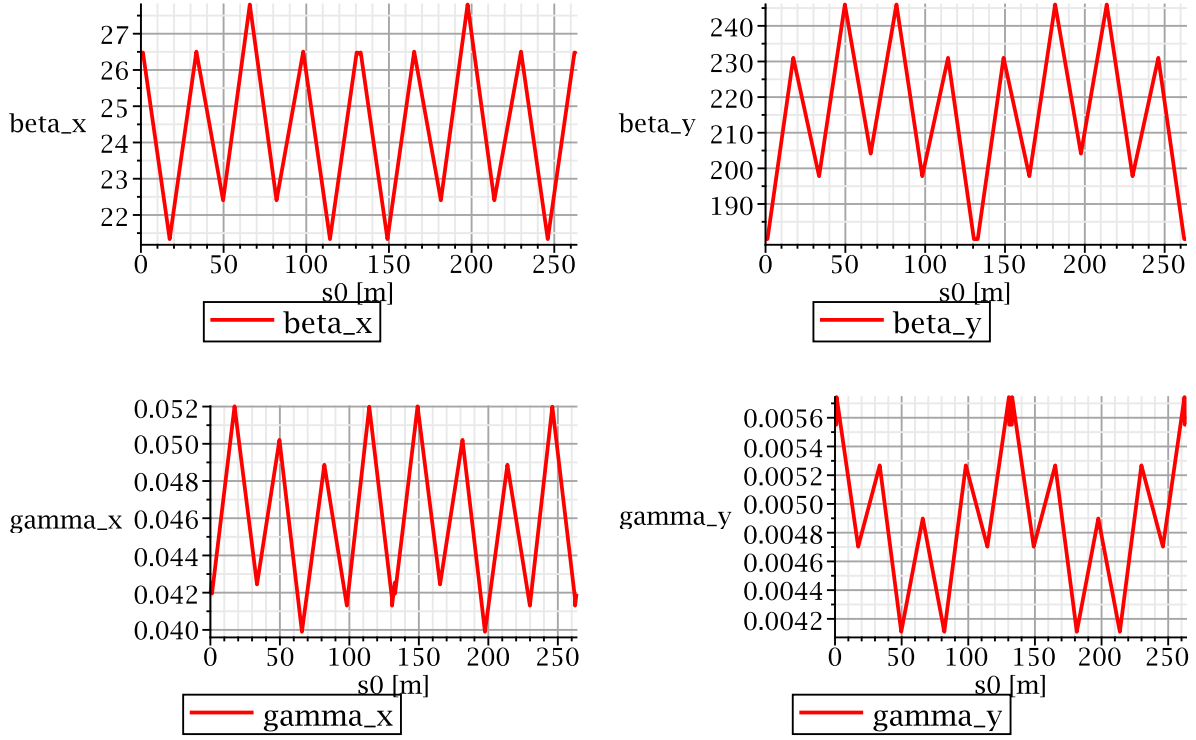


Figure 7: Plots of β and γ functions of (almost round) racetrack-shaped proton EDM lattice. β_y is *necessarily* very large, since Q_y **has to be small**. γ_y has to be very small to reduce spin decoherence due to vertical betatron oscillations.

6.2 “All-In-One” Lattice for Measuring p , d , and ${}^3\text{He}$

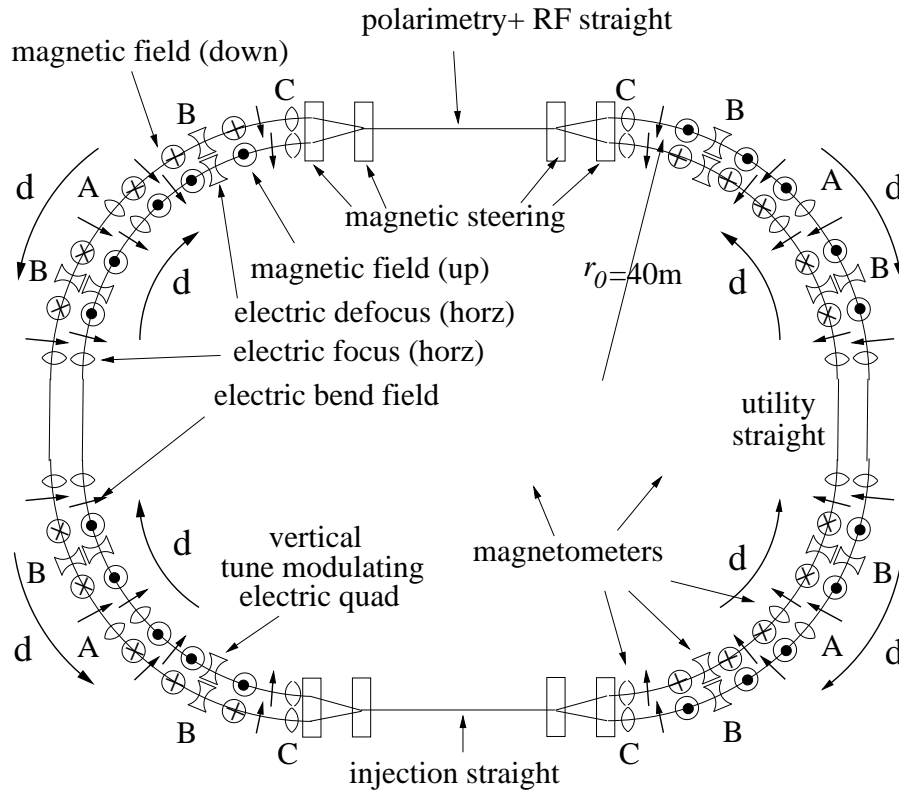


Figure 8: “All-In-One” lattice for measuring EDM’s of protons, deuterons, and helions.

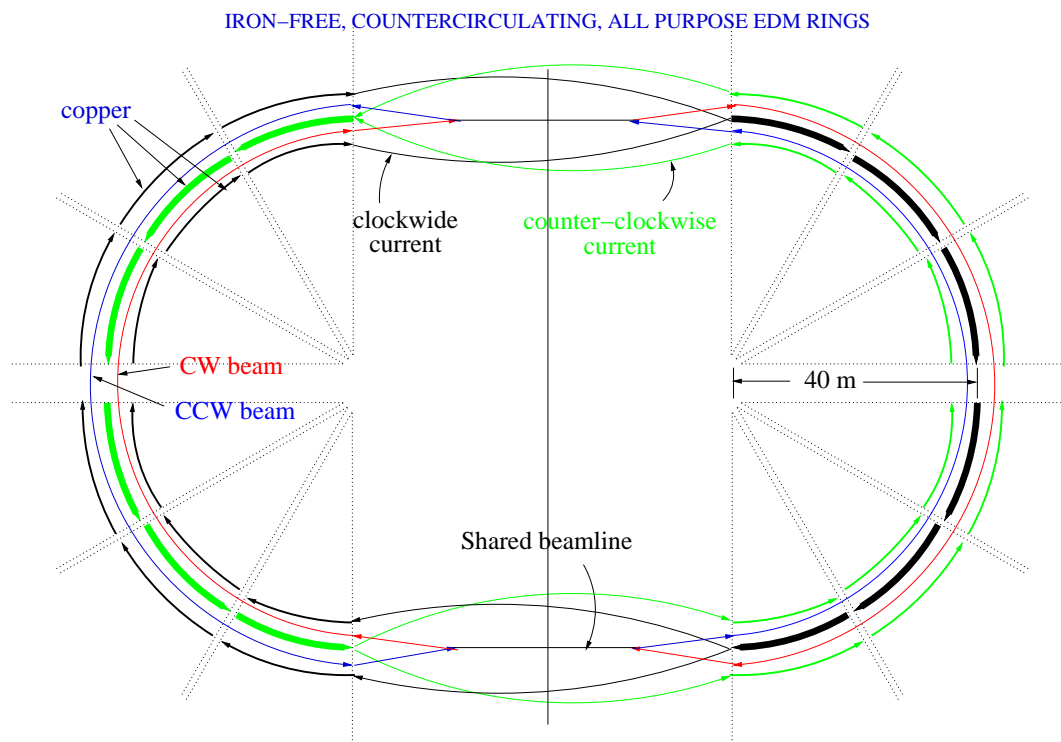
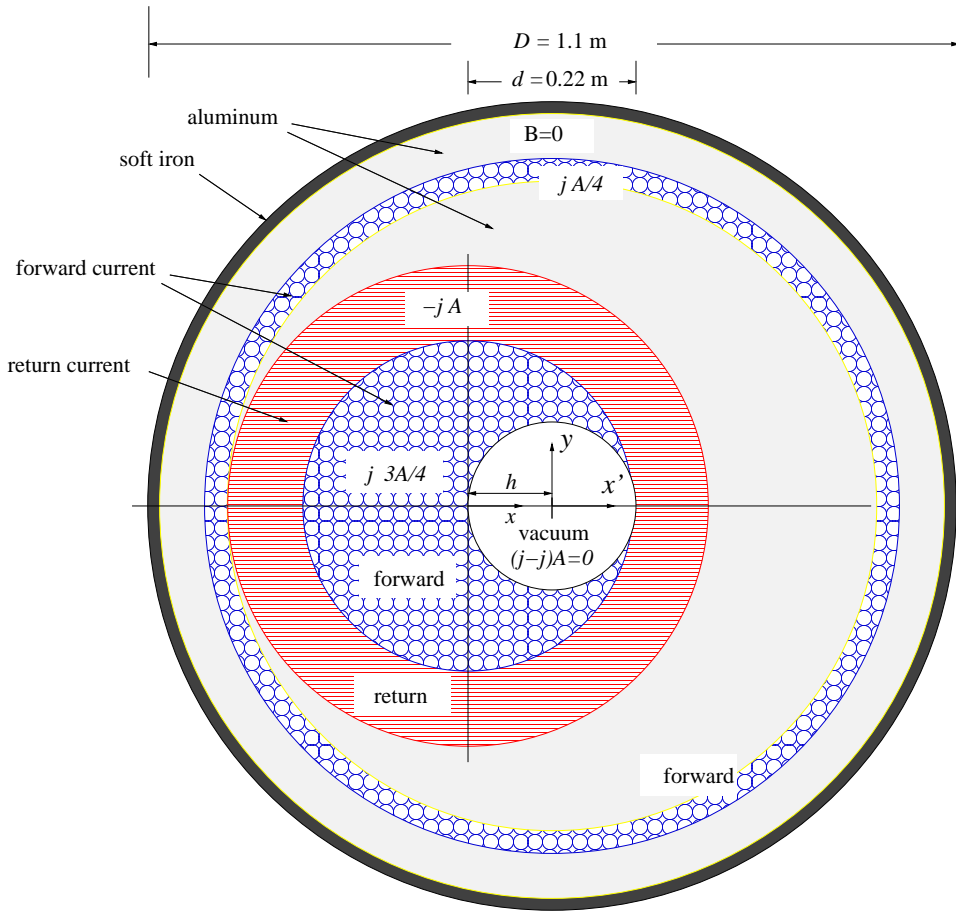


Figure 9: Universal, interleaved storage rings constructed from iron-free, current-only magnets for EDM measurements using counter-circulating beams with electric and/or magnetic deflection—**An all-septum storage ring.**



Return tube of current and outer forward tube of current give no magnetic field in vacuum region

No hole:

$$B'_x = -\frac{\mu_0 j}{2} y$$

$$B'_y = \frac{\mu_0 j}{2} x$$

Anti-hole:

$$B''_x = \frac{\mu_0 j}{2} y$$

$$B''_y = -\frac{\mu_0 j}{2} x'$$

No hole + Anti-hole:

$$B_x = B'_x + B''_x = 0$$

$$B_y = B'_y + B''_y = \frac{\mu_0 j}{2} (x - x') = \frac{\mu_0 j h}{2}$$

Assumed maximum magnetic field: $B_{\max} = 0.15 \text{ T}$

Assumed maximum current density: $j_{\max} = 2 \times 10^6 \text{ A/m}^2$

$$h = \frac{2B}{\mu_0 j} = \frac{2 \times 0.15}{4\pi \times 10^{-7} \times 2 \times 10^6} = 0.119 \text{ m}$$

Figure 10: Iron-free, all current, uniform field magnet. The current configuration starts from an example in Landau and Lifshitz, *Electrodynamics of Continuous Media*.

6.3 All-electric Ring In Tevatron Accumulator Tunnel

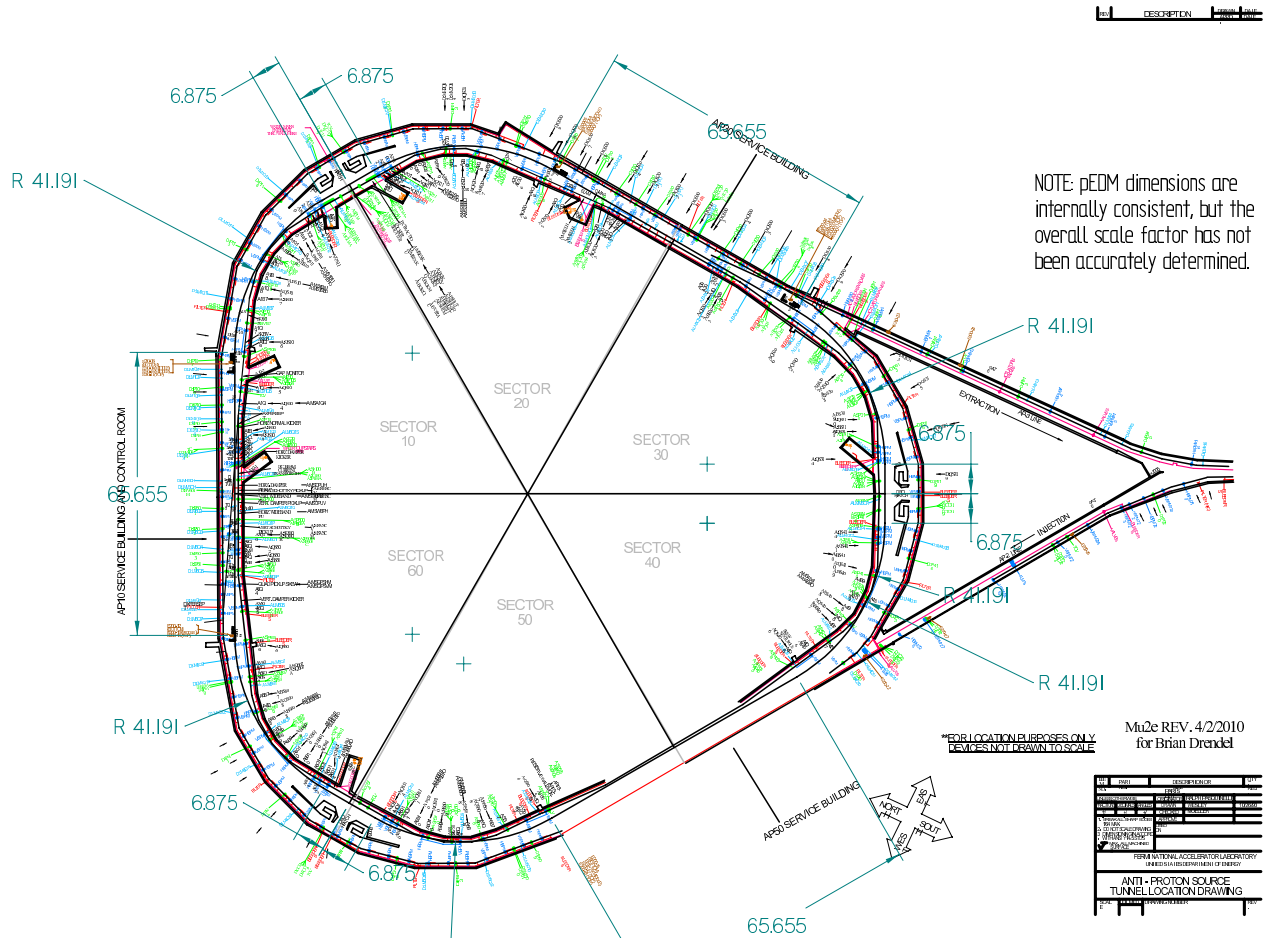


Figure 11: The pEDM ring stands on the footprint of the Tevatron Accumulator.

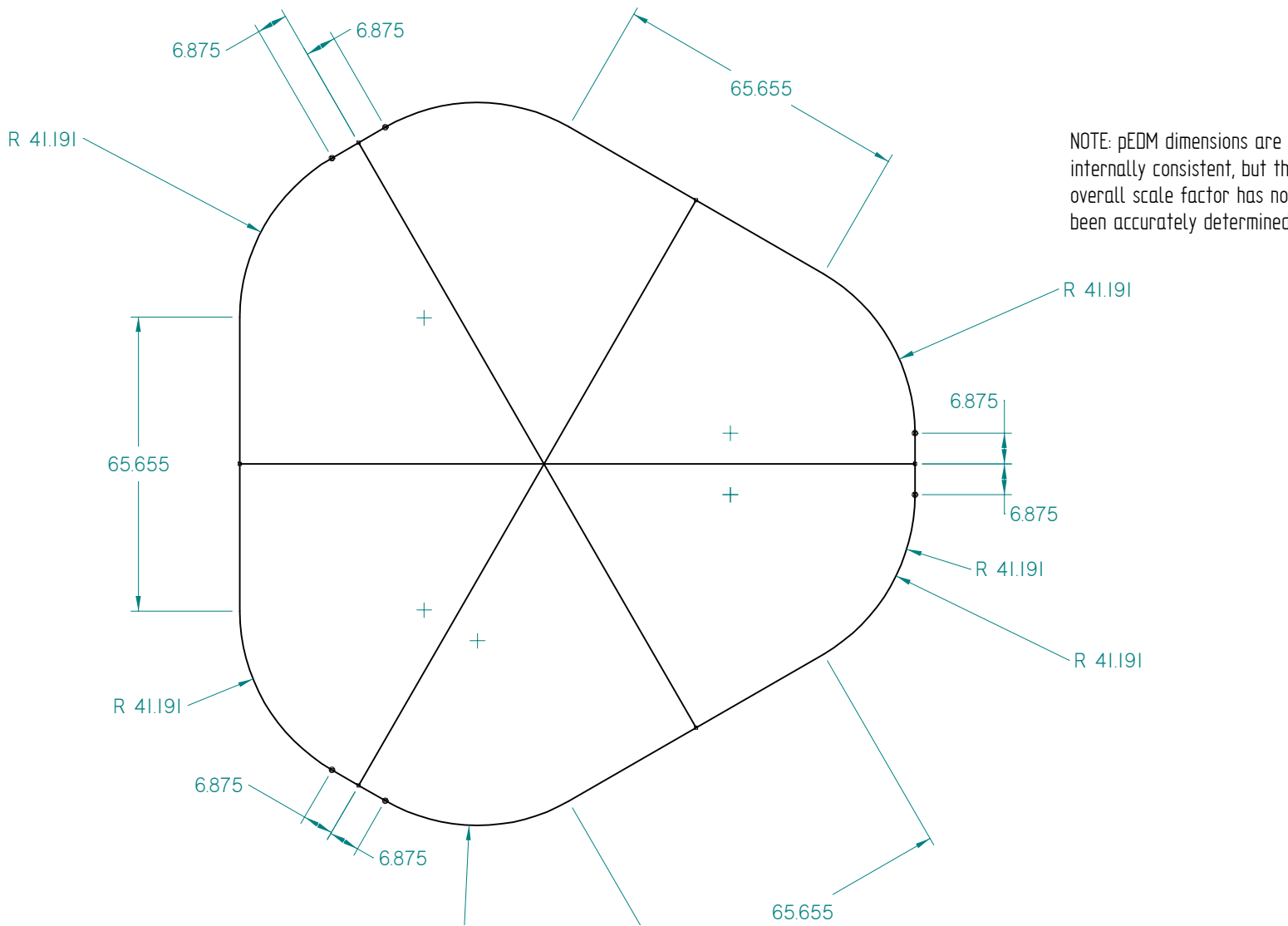


Figure 12: Geometry of the design orbit of the all-electric proton EDM ring in the Tevatron accumulator tunnel.

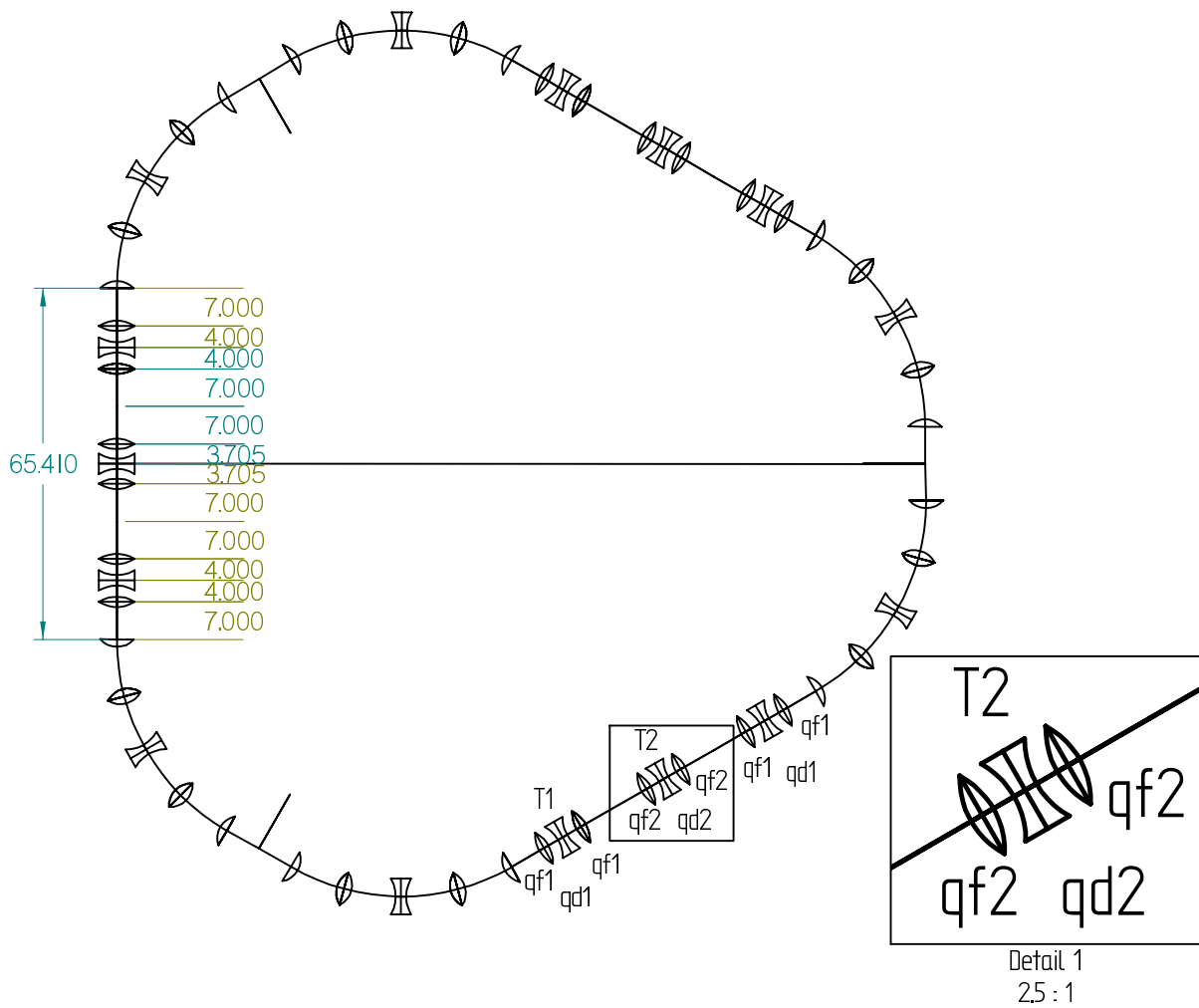


Figure 13: Focusing optics of the all-electric proton EDM ring in the Tevatron accumulator tunnel. The long straight sections are matched by a triplet of triplets (T1, T2, T1). The dimensions are not exactly as shown. For example all triplet separations are actually equal (to 4.0 m). Also the sub-elements of T2 have polarities opposite to what their names suggest.

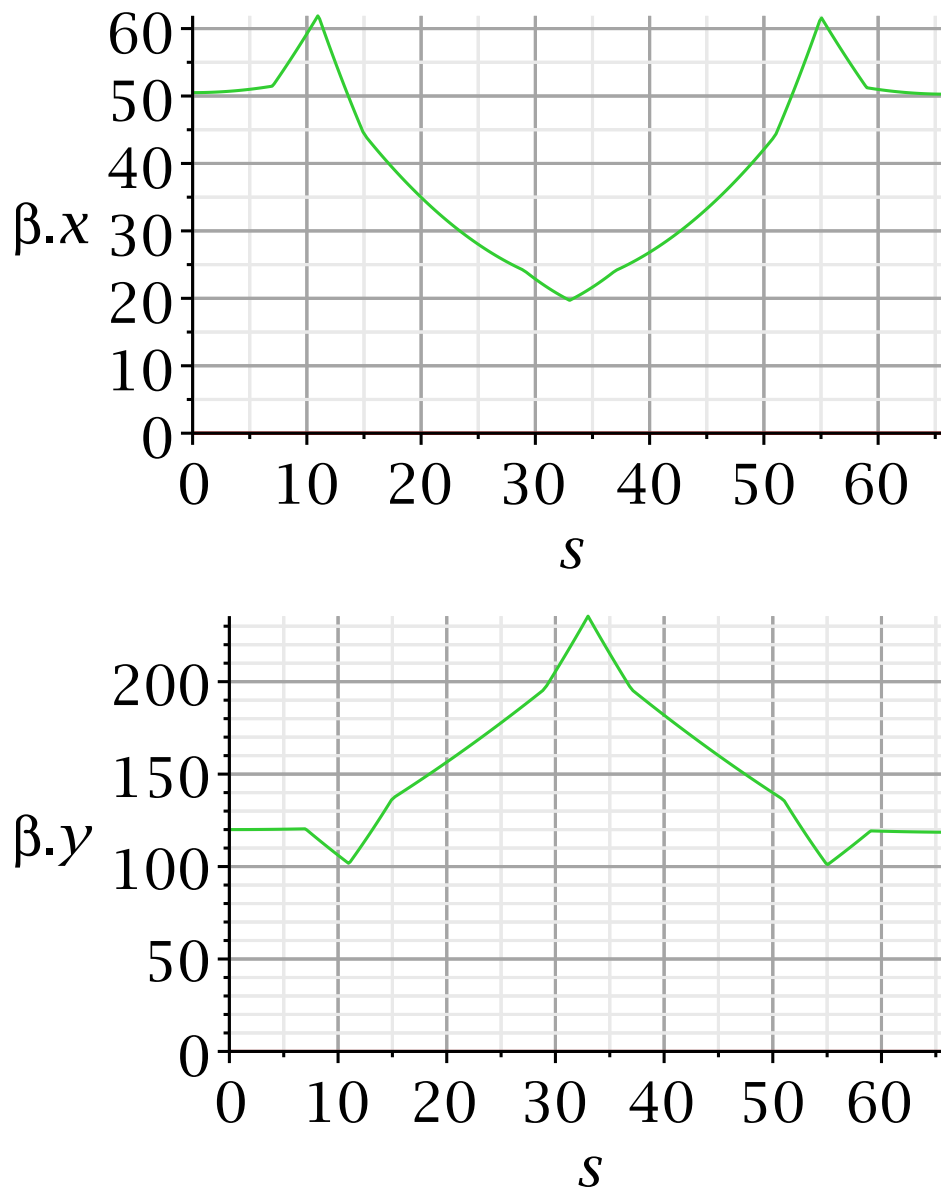


Figure 14: β -functions (in meters) in long straight sections for the proton EDM ring in the Tevatron accumulator tunnel.

7 COSY Storage Ring Test Using Tevatron Electrostatic Separator

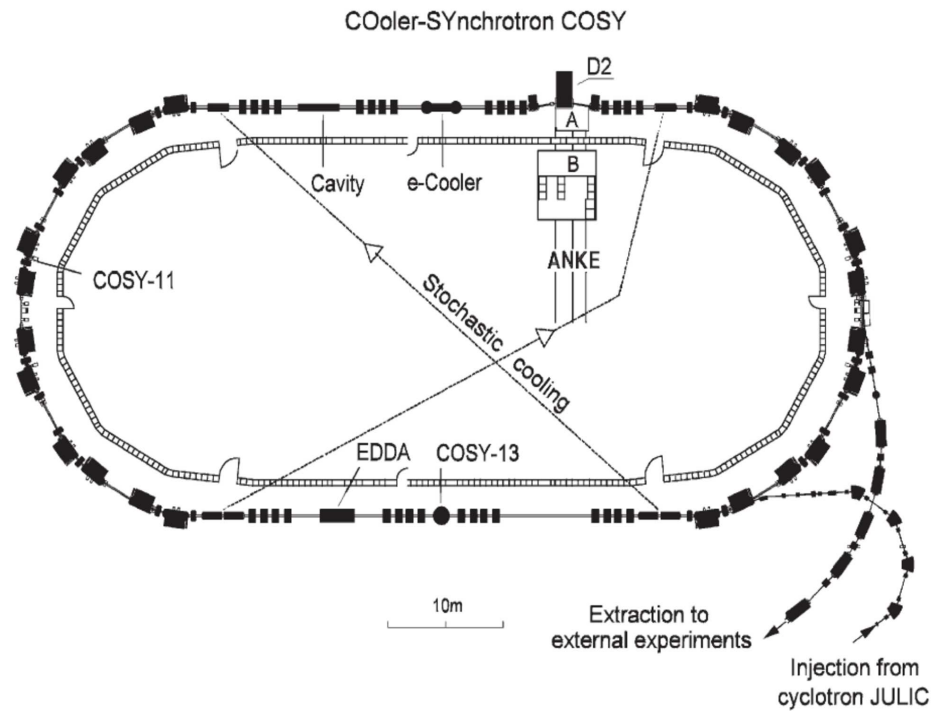


Figure 15: The COSY ring. The ANKE experiment is on rails and could be removed temporarily to be replaced by the B-E-B chicane.

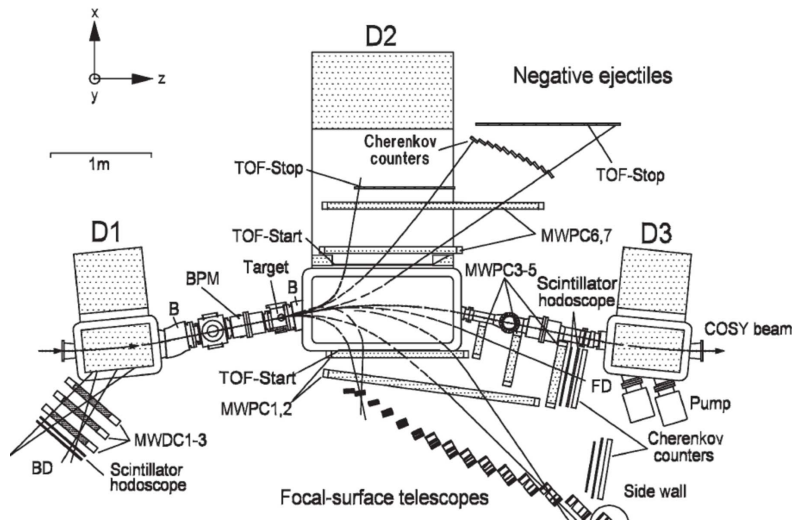


Figure 16: The ANKE experimental region. Dipole D2 and adjacent equipment are to be replaced by the Tevatron electric separator. Dipoles D1 and D3 provide the magnetic bends of the B-E-B chicane.

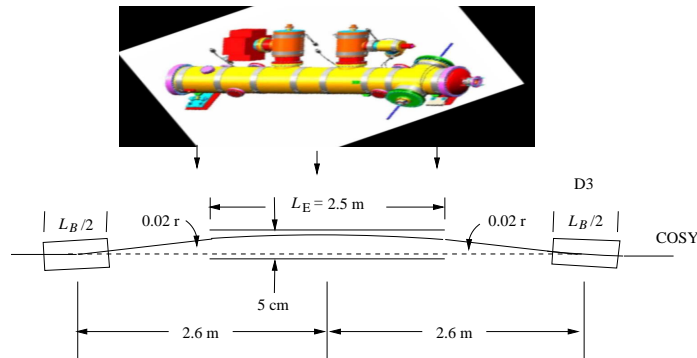


Figure 17: The Tevatron electrostatic separator (drawn roughly to scale) will form the central element of the B-E-B chicane. Here the separator is positioned for one-sided operation.

8 Essentials for any Hadron EDM Measurement

The following considerations largely dictate the requirements for, and the design of, storage ring lattices for EDM measurements.

- Beam quality:

Intense, low emittance source of highly polarized particles. Counting statistics of polarimetry dominate statistical error and **polarimetry consumes stored particles**, limiting the lengths of runs.

High efficiency and polarization preservation during injection.

Post-injection electron beam cooling can be used (for longer spin coherence time) but must be turned off for entire data collection time.

Stochastic beam cooling (if possible) could be used during data run.

- **Maximal radial electric field E_r** , since the EDM signal is proportional to E_r .

- **High analyzing power polarimetry.** This constrains the beam energy. Fortunately the analyzing power of proton-carbon scattering is near optimal at the proton magic energy.
- **Multiple circulating bunches of alternating polarization,** forward and back (to cancel polarimetry asymmetries).
- Frozen longitudinal polarization (so EDM effect accumulates). This requires **closed-loop polarimeter/RF frequency feedback.** This capability is right now being developed at COSY!

- **Several orders of magnitude suppression of magnetic field** (because, radial magnetic field acting on the magnetic moment, mimics the EDM signal). This requires using both passive magnetic shielding and active B_r correction coil.

- **Counter-circulating beams:**

Measure the difference between vertical spin precession of counter-circulating beams (to avoid having to determine absolute spin precession of either beam).

Extremely **precise vertical beam position measurement**. Any vertical deviation of counter-circulating beams is due to radial magnetic field acting on EDM. This amounts to being model-independent cancellation of MDM precession by cancelling relative vertical displacement of the two beams. BPM inaccuracy will probably dominate the ultimate systematic error on the measurement.

Squid magnetometers are currently thought to be the best option. In controlled lab environment they have been shown to provide the needed accuracy. But they have to function in the (noisy) accelerator environment.

- Modulating Q_y at fixed frequency in the kHz range modulates the beam separation at a frequency chosen to be in a low noise region of the spectrum. **Synchronous, lock-in detection** of the vertical beam separation permits greater BPM accuracy than is possible with conventional storage rings.

- **Low vertical tune**, e.g. $Q_y \approx 0.1$, is favored for various reasons:

Mainly, to improve the precision with which the average $\langle B_r \rangle$ can be suppressed toward zero. The **modulated vertical beam separation** is proportional to $1/Q_y$.

Contribution of vertical betatron oscillation to **spin decoherence is proportional to γ_y** . This requires β_y to be large and α_y to be small. The latter forces Q_x to also be fairly small.

- **Regular reversals** of field strengths and circulation directions to cancel systematic errors.

With all-electric bending the counter-circulating beams superimpose exactly, and optical properties are identical for the two beams.

For the all-electric ring reversing the beam directions is equivalent to doing nothing (or, at most, cancelling injection asymmetry.)

For magnetic bending the beams have to be separated and their optical properties will therefore not be identical. In compensation for this, with separated beams, the fields and circulation directions can be reversed, which cancels many systematic errors.

For the all-purpose ring, reversing ring traversals is both possible, *and necessary*.

- **Hysteresis rules out both iron-dominated and superconducting magnets.** There is no protection against field reversal effects that cannot be understood experimentally.

9 Orbits in Electric Fields

9.1 Synchro-Betatron Coupling

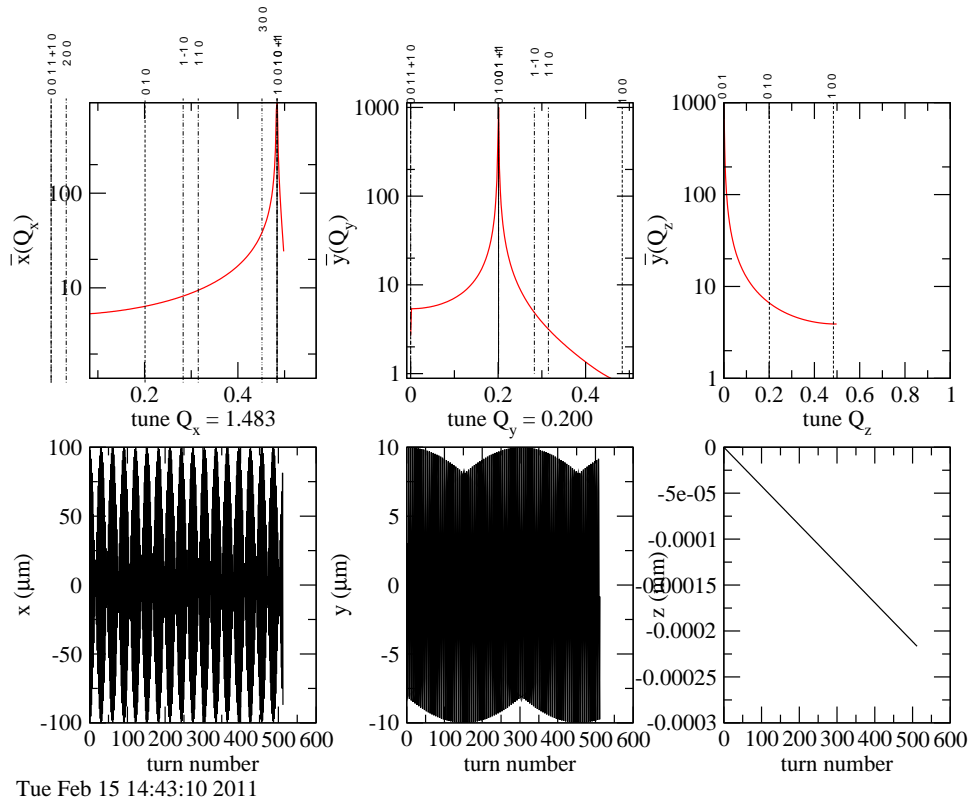


Figure 18: Coarse resolution tracking results for simultaneous vertical and horizontal motion of one particle in an idealized “first test” ring.

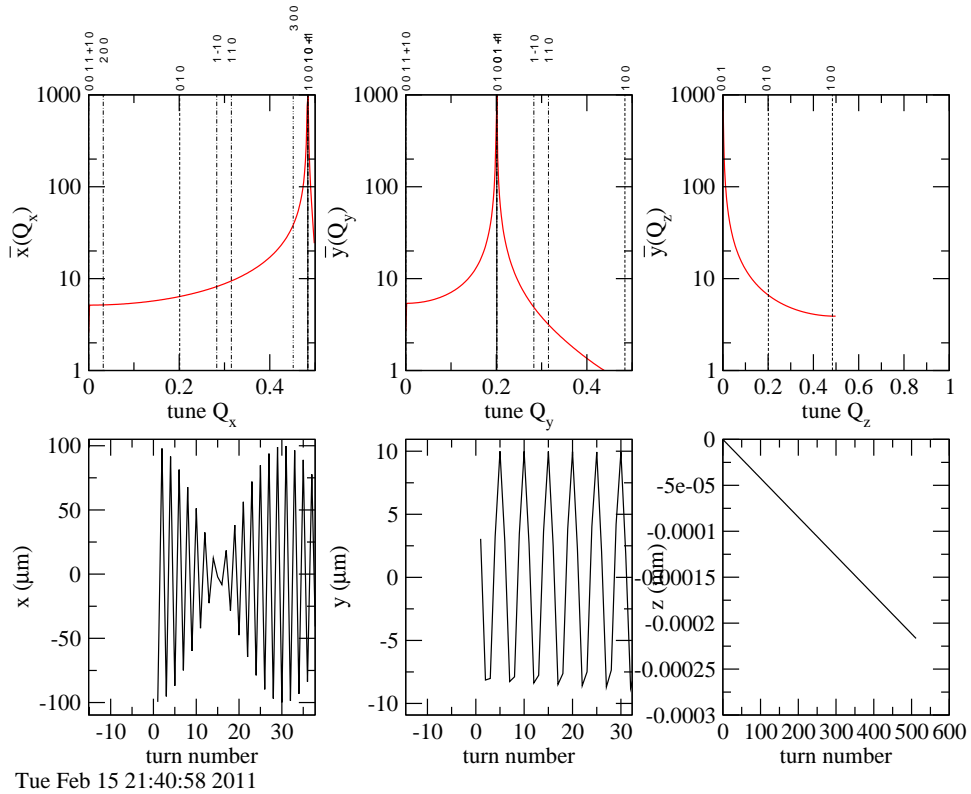


Figure 19: Fine resolution version of Figure 18. Only a brief time interval is displayed so that individual turns can be observed.

9.2 “Exact” Tracking with UAL/ETEAPOT Code

- An electric field with index m power law dependence on radius r for $y=0$ is

$$\mathbf{E}(r, 0) = -E_0 \frac{r_0^{1+m}}{r^{1+m}} \hat{\mathbf{r}}, \quad (11)$$

and the electric potential $V(r)$, adjusted to vanish at $r = r_0$, is

$$V(r) = -\frac{E_0 r_0}{m} \left(\frac{r_0^m}{r^m} - 1 \right). \quad (12)$$

- The “cleanest” case has $m=1$, in which case it is known as the Kepler or the Coulomb electric field, except we must use **relativistic mechanics**.
- Remarkably, the **exact solution in 2D can be expressed in closed form for arbitrary amplitude**.
- The actual field index value will have $m \neq 1$. For long term tracking we use exact (and hence symplectic) $m=1$ evolution but “**kick correct**” (also symplectic) to the actual m value.

- The **total energy**

$$\mathcal{E} = eV(\mathbf{r}) + \gamma(\mathbf{r})m_p c^2, \quad (13)$$

(rather than just the second term), is conserved (except for tiny changes each passage through RF cavities.) So recalculate $\gamma(\mathbf{r})$ whenever it is needed (e.g. to use Lorentz force to obtain acceleration.)

- The **angular momentum** is

$$\mathbf{L} = \mathbf{r} \times \mathbf{p}. \quad (14)$$

- Both \mathcal{E} and \mathbf{L} are constants of the motion, **but β and γ are not.**
- **Courant-Snyder, Twiss function formalism breaks down within electric elements**, but can be consistently maintained outside electric elements (and then interpolated through them).

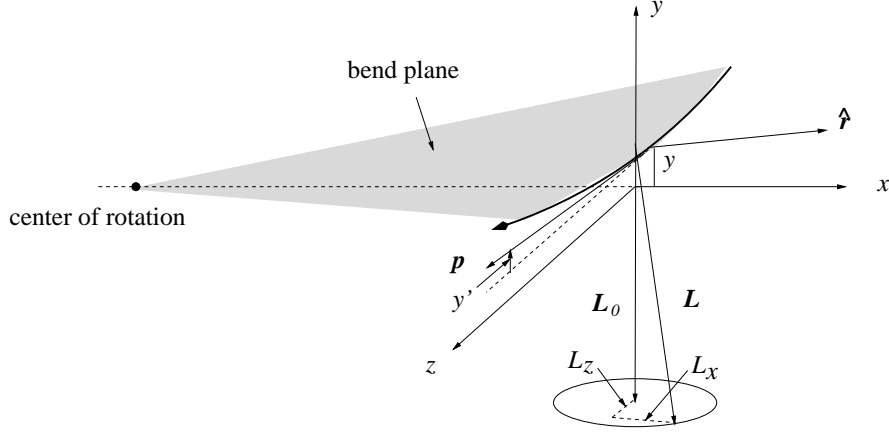


Figure 20: Wobbling-plane orbit coordinate definitions.

- For transverse orbit description, replace Courant-Snyder 4D phase space description by wobbling plane description. Instead of (x, x', y, y') Courant-Snyder (Frenet) coordinates, use $(x \rightarrow \Delta r, x' \rightarrow \Delta r', y \rightarrow -L_z, y' \rightarrow L_x)$ displacements.
- The phase space pair (L_x, L_z) rather than the pair (y, y') are evolved. But, if re-scaled appropriately, to linear order, the numerical values are the same. See table.

Table 1: Transfer-matrix-preserving redefinitions of the phase space coordinates.

coord. indexed	MAD and UAL and TEAPOT			ETEAPOT, drift/kick			Muñoz-	Pavic	bend/kick
	coord. concept.	coord. scaled	coord. linear.	coord. concept.	coord. scaled	coord. linear.	coord. concept.	coord. scaled	coord. linear.
p[0]	\bar{x}	\bar{x}	\bar{x}	x	$x = r_0 - r$	$\approx \bar{x}$	h_θ	$-\beta^2 h_\theta / r_0$	$\approx \bar{x}$
p[1]	\bar{p}_x	\bar{p}_x / p_0	$\bar{x}' \approx \bar{\theta}_x$	p_r	p_r / p_0	$\approx \bar{p}_x / p_0$	h_r	h_r	$\approx \bar{p}_x / p_0$
p[2]	\bar{y}	\bar{y}	\bar{y}	\bar{L}_x	$r_0 \bar{L}_x / \bar{L}$	$\approx \bar{y}$	\bar{L}_x	$r_0 \bar{L}_x / \bar{L}$	$\approx \bar{y}$
p[3]	\bar{p}_y	\bar{p}_y / p_0	$\bar{y}' \approx \bar{\theta}_y$	\bar{L}_z	$-\bar{L}_z / \bar{L}$	$\approx \bar{p}_y / p_0$	\bar{L}_z	$-\bar{L}_z / \bar{L}$	$\approx \bar{p}_y / p_0$
p[4]	Δt	$-\Delta z / v$		Δt	$-\Delta z / v$		Δt	$-\Delta z / v$	
p[5]	$\Delta \mathcal{E}$	$\Delta \gamma m_p c / p_0$		$\Delta \mathcal{E}$	$\Delta \mathcal{E} / (p_0 c)$		$\Delta \mathcal{E}$	$\Delta \mathcal{E} / (p_0 c)$	

10 Estimation of Spin Coherence Time (SCT)

- Uniform, weak focusing lattice with no drift regions. SCT is hopelessly short for “coasting beams”, but not for “bunched beams”.

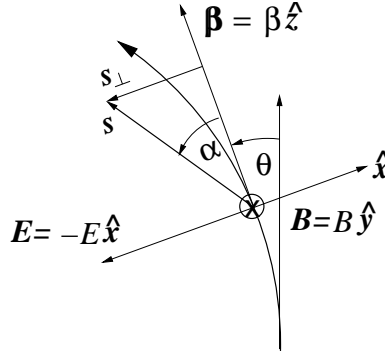


Figure 21: Spin vector \mathbf{s} has precessed through angle α away from its nominal direction along the proton’s velocity, as the beam direction has evolved through angle θ .

- MDM torque causes spin precession angle α to evolve;

$$\frac{d\alpha}{dt} = \frac{eE(x)}{m_p c} \left(\frac{g\beta(x)}{2} - \frac{1}{\beta(x)} \right). \quad (15)$$

- This vanishes for particles at the magic velocity but not for off-momentum particles. Synchrotron oscillations tend to cancel on the average, but the averages $\langle g\beta/2 \rangle$ and $\langle 1/\beta \rangle$ are typically unequal.

- Synchrotron oscillations are most naturally expressed in terms of “energy” γ rather than β

$$\left\langle \frac{d\alpha}{d\theta} \right\rangle = \left\langle \frac{eE(x)(r_0 + x)^2}{Lc\beta(x)} \right\rangle \left(\left(\frac{g}{2} - 1 \right) \langle \gamma(x) \rangle - \frac{g}{2} \left\langle \frac{1}{\gamma(x)} \right\rangle \right). \quad (16)$$

- The first factor can be treated as constant. For typical energy spreads, if the second factor is of order 1, the spin coherence time would be SCT \sim milliseconds.
- The first term of the second factor vanishes after synchrotron oscillation averaging but, in general, the second does not.
- A virial theorem with “virial” G is defined by

$$G = \mathbf{r} \cdot \mathbf{p} \quad (17)$$

can be used to perform the averaging.

- Evaluate dG/dt using Newton’s law for our electric field;

$$\mathbf{E} = -E_0 \left(\frac{r_0}{r} \right)^{1+m} \hat{\mathbf{r}}. \quad (18)$$

- Averaging over time, and presuming bounded motion (so G remains bounded) one obtains

$$\left\langle \frac{1}{\gamma} \right\rangle = \langle \gamma \rangle - \frac{E_0 r_0}{m_p c^2 / e} \left\langle \frac{r_0^m}{r^m} \right\rangle. \quad (19)$$

- Applying this result to average Eq. (16) yields

$$\left\langle \frac{d\alpha}{d\theta} \right\rangle \approx -\frac{E_0 r_0 \gamma_0}{(p_0 c / e) \beta_0} \left(\left\langle \frac{\gamma}{\gamma_0} - 1 \right\rangle + m \left\langle \frac{x}{r_0} \right\rangle - \frac{m^2 - m}{2} \left\langle \frac{x^2}{r_0^2} \right\rangle + \dots \right). \quad (20)$$

- Polarimeter/RF frequency feedback cancels the first term exactly.
- The terms vanish for $m = 0$.
- Since x/r_0 is of order 2×10^{-4} , terms not shown can be neglected.
- For $m = 1$ the final term vanishes. For small energy spread and careful nonlinear lattice design it may be possible to cancel the $\langle x \rangle$ term adequately.